Editors' Suggestion

Femtosecond Timekeeping: Slip-Free Clockwork for Optical Timescales

D. Herman,[1,2] S. Droste,[1] E. Baumann,[1] J. Roslund,[3] D. Churin,[3] A. Cingoz,[3] J.-D. Deschênes,[4] I. H. Khader,[1] W. C. Swann,[1] C. Nelson,[1] N. R. Newbury,[1] and I. Coddington[1,*]

[1]*National Institute of Standards and Technology, 325 Broadway, Boulder, Colorado 80305, USA*
[2]*Department of Physics, University of Colorado Boulder, Boulder, Colorado 80309, USA*
[3]*AOSense Inc., 929 East Arques Avenue, Sunnyvale, California 94085, USA*
[4]*Université Laval, 2325 Rue de l'Université, Québec City, Québec G1V 0A6, Canada*

(Received 16 August 2017; revised manuscript received 18 December 2017; published 3 April 2018)

The generation of true optical time standards will require the conversion of the highly stable optical-frequency output of an optical atomic clock to a high-fidelity time output. We demonstrate a comb-based clockwork that phase-coherently integrates $\sim 7 \times 10^{20}$ optical cycles of an input optical frequency to create a coherent time output. We verify the underlying stability of the optical timing system by comparing two comb-based clockworks with a common input optical frequency and show <20 fs total time drift over the 37-day measurement period. Both clockworks also generate traditional timing signals including an optical pulse per second and a 10-MHz rf reference. The optical pulse-per-second time outputs remain synchronized to 240 attoseconds (240 as) at 1000 s. The phase-coherent 10-MHz rf outputs are stable to near a part in 10^{19}. Fault-free timekeeping from an optical clock to femtosecond level over months is an important step in replacing the current microwave time standard by an optical standard.

DOI: 10.1103/PhysRevApplied.9.044002

I. INTRODUCTION

Over the last decade, optical clocks have been demonstrated to be the future of timekeeping. Lattice and ion-based optical clocks provide several orders of magnitude higher frequency stability than the best microwave-based standards, while low-noise optical oscillators, such as stabilized lasers, now outperform their quietest radio-frequency (rf) analogs [1–5]. Alternatively, atomic vapor-cell optical clocks have the potential to rival current microwave clocks, but with a significantly smaller form factor [6–8]. Such clocks could be used, for example, in the next generation of global positioning satellites. Additionally, optical time and frequency transfer is now available to compare and synchronize these standards at high levels of stability [9–12]. While the exact form of an optical time standard has not been finalized, all contenders must convert their optical frequency—oscillating in the hundreds to thousands of terahertz to a usable timing signal, typically a single pulse per second (PPS).

When properly phase locked, a frequency comb provides exactly this "clockwork" function, converting the femtosecond-scale ticks of the optical reference to the nanosecond-scale ticks of the comb's optical pulse train. However, the frequency comb introduces two optical phase locks into the system: the carrier-envelope-offset lock and the lock to the optical clock frequency [13]. A single cycle (phase) slip in either introduces a random and potentially significant time offset. Phase-locked frequency combs have traditionally operated without phase slips for hours, or occasionally days, but not months or years [14–16]. We note that the transfer-oscillator approach to frequency comb metrology [17], while simpler, will not provide clockwork functionality.

One way to avoid phase slips is to produce a coherent time output using a hydrogen maser, which has a negligible phase-slip rate, as a flywheel that is steered by an optical clock frequency reference [18,19]. However, the maser can limit the hypothetical performance of ultrastable optical timescales and is immediately problematic for clocks targeting low-size and low-power operation [6–8]. Here, we directly address the cycle-slip problem so that the frequency comb itself provides the usable timescale—in this case, a PPS and rf output. This approach provides a simple and direct method to convert optical atomic frequency standards to timescales. It could support the generation of time either from a combination of a high-performance optical clock and associated optical flywheel (when such systems mature to continuous operation) or directly from a compact vapor-cell optical atomic clock [6–8].

By combining new, robust comb architectures and field-programmable gate-array (FPGA)-based locking electronics, we demonstrate two sets of comb-based optical clockwork that operate without timing errors for over a month. Each clockwork is locked to a common optical-frequency reference and generates a 160-MHz

*ian.coddington@nist.gov

optical pulse train, an optical PPS, and a traditional 10-MHz rf reference. Time offsets for both optical signals are measured for 37 days. In that period, the relative timing of the pulse trains wander 18.5 fs and the relative timing of the PPS wanders approximately 265 fs. Importantly, we verify the absence of cycle slips in the 37-day data set. The demonstration ends when one frequency comb slowly drifts into a software-defined limit on its pump current feedback, causing the carrier-envelope-offset frequency (f_{CEO}) to unlock. Further comb engineering or phase-coherently transferring timing information to redundant combs—as is often done with masers—allows one to greatly extend the performance period.

II. EXPERIMENT AND RESULTS

A schematic of the experimental setup is shown in Fig. 1(a). Each clockwork system is based on an f_{CEO}-stabilized frequency comb with a repetition rate of 160 MHz. We use a low-noise fiber-laser frequency comb from AOSense, incorporating an all-polarization-maintaining fiber design with saturable absorber-based mode locking based loosely on Ref. [16]. A fast piezo-electric transducer cavity-length actuator with 90° phase roll-off at ~500 kHz counteracts environmental perturbations. To probe the performance of the clockwork itself, each comb is locked to a common cavity-stabilized cw laser yielding a pulse-to-pulse timing jitter of 1 fs. The cw laser operates as a proxy optical clock, with a wavelength of 1565 nm (191 THz) and Hz-level linewidth. The cavity is not referenced to an atomic transition and drifts several kHz per day. To ensure a single time base, each comb is fully self-referenced and the FPGA locking electronics are clocked off the comb repetition rates.

The main obstacle for comb-based clockwork (or any true time-scale generator) is the presence of cycle slips. There are two distinct sources of slips that must be confronted. First, for a given SNR of a detected lock frequency, there is a finite probability that even an ideal phase-locked loop will either miss or falsely detect a cycle, introducing a single optical cycle of timing error. Fortunately, this probability falls off exponentially with increasing SNR and, with care, the probability of a cycle slip becomes negligible [16]. Second, external perturbations will potentially disrupt the clockwork's locks. If the perturbation is sufficiently large, it can unlock the system altogether, or cause a random cycle slip. The impact of these disruptions can be mitigated by environmental isolation and the use of robust, all-fiber combs [16,20–24]. Unfortunately, momentary losses of phase lock are hard to eliminate completely. Historically, comb-based frequency comparisons have ignored this problem, since these slips

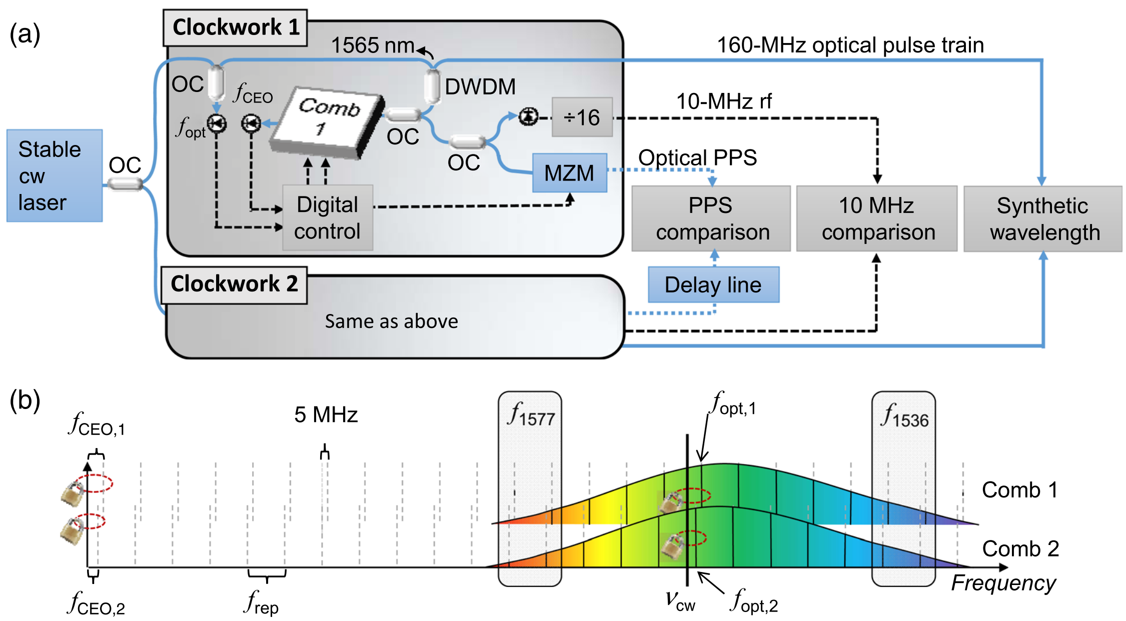

FIG. 1. (a) Experimental setup. Each comb-based clockwork converts the common optical frequency of 191 THz (ν_{cw}) to three outputs: (1) a 160-MHz optical pulse train, (2) an optical PPS signal, and (3) a 10-MHz rf output. To evaluate the clockwork performance, we compare these three outputs of the two clockworks, as discussed in the text. (b) Phase-locking scheme to enable the timing comparison. All lock frequencies between the combs are the same sign but offset such that $f_{\mathrm{CEO},1} - f_{\mathrm{CEO},2} = f_{\mathrm{opt},1} - f_{\mathrm{opt},2} = 5$ MHz. The shaded regions labeled f_{1577} and f_{1536} indicate the bands used for the synthetic wavelength measurement (direct comparison of two optical pulse trains). OC, optical coupler; DWDM, dense wavelength division multiplexer; MZM, Mach-Zehnder modulator, "÷16," rf divider; f_{CEO}, carrier-envelope offset frequency; f_{opt}, offset frequency between the cw laser and one optical comb tooth; f_{rep}, comb repetition rate.

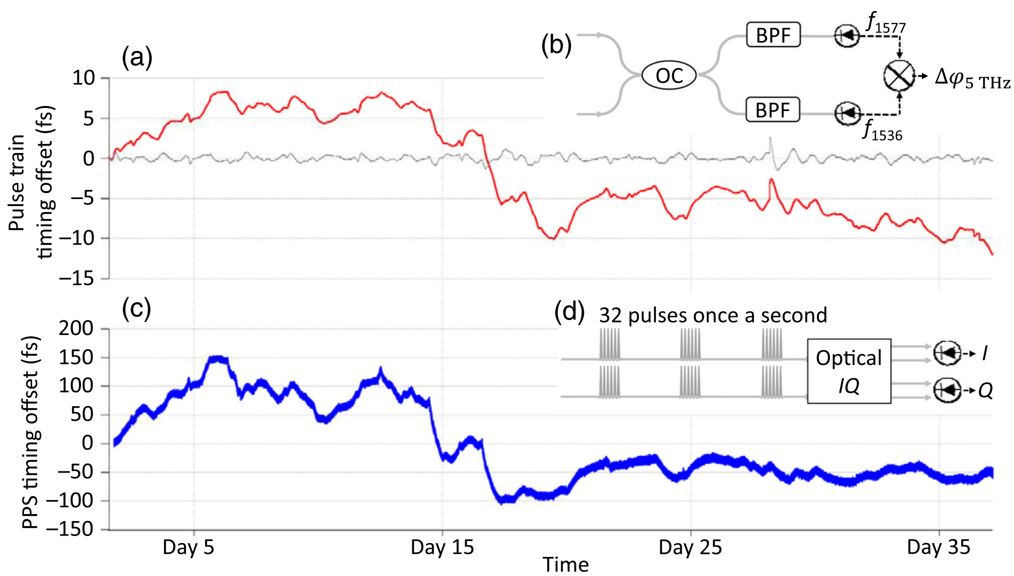

FIG. 2. (a) Time offset between the two optical pulse trains (red line) as measured for 37 days using the synthetic wavelength technique. After high-pass filtering (gray line) the data show the clear absence of phase slips. (b) Setup of the pulse-train optical timing comparison. BPF, optical band-pass filter. (c) Time offset between the PPS clock outputs (blue line) over the same 37-day period. (d) Setup of the PPS optical timing comparison.

can be identified and removed from their data [14]. However, a random loss of timing information cannot be tolerated in a timescale.

We address the problem of transients by employing a digital phase-locked loop implemented on an FPGA [16]. The main benefit of digital locking is an increased phase-coherent recapture range. As the lock signal's phase is extracted digitally, one can unwrap and track phase excursions up to 2^{48} radians—a dynamic range many orders of magnitude beyond that possible with rf electronics [16,25]. Thereby, the loss of timing information is prevented and effectively infinite phase tracking is maintained, provided that the detected signal frequency falls within the detection bandwidth of 50 MHz.

As shown in Fig. 1(a), the clockworks each produce three outputs. We verify slip-free performance by comparison of the 160-MHz optical pulse trains. This approach provides a very sensitive measurement of the underlying comb timing, as discussed in Sec. II A, but only for excursions between 10 as and 100 fs. For an actual time output, we generate an optical PPS signal—described in Sec. II B—capable of tracking timing shifts from 1 fs to 1 s. Finally, the 10-MHz rf output comparison is discussed in Sec. II C.

A. Optical pulse-train timing comparison

The relative time offset of the 160-MHz optical pulse trains is compared, using the heterodyne technique described in Ref. [26]. This approach works by comparing the differential optical phase between the combs at two points in the comb spectrum, separated by 5 THz. As shown in Figs. 1 and 2(b), the combs are offset by 5 MHz and two filtered bands at 1536 nm (195 THz) and 1577 nm (190 THz) are heterodyned to create 5-MHz tones (f_{1536}, f_{1577}), which are electronically mixed to yield the phase shift, $\Delta\varphi_{5\ \mathrm{THz}} = 2\pi(5\ \mathrm{THz})\Delta t$, where Δt is the relative timing shift between the clockworks. $\Delta\varphi_{5\ \mathrm{THz}}$ is filtered to a 3-Hz bandwidth and sampled at 10 Hz. We achieve a ~20 fs/V timing sensitivity after amplification and reach a noise floor of 2 as. As detailed in Ref. [26], this approach provides excellent sensitivity to optical timing shifts over a broad range with a relatively simple setup.

Figure 2(a) shows the time offset between the pulse trains, measured continuously over 37 days. The peak-to-peak wander is 18.5 fs. The slow wander is attributed to variations in the differential fiber path length within the two clockworks due to environmental perturbations (see next subsection). If either comb missed a single optical cycle, there would be a ±5 fs instantaneous jump in the relative timing. To verify that no such slips occurred, we remove the slow timing wander by high-pass filtering the timing data with a corner frequency of 10^{-4} Hz. The result, plotted in gray in Fig. 2(a), shows no timing excursion larger than 2 fs, verifying the absence of cycle slips for the entire 37-day period.

B. Optical PPS timing comparison

Typical commercial microwave clocks, such as hydrogen masers and GPS-steered rubidium standards, are equipped with a PPS, providing an unambiguous timing signal for comparing or synchronizing clocks. Here, we demonstrate an optical PPS which provides a similar unambiguous timing signal but with subfemtosecond precision capable of supporting modern optical clocks.

To create the PPS, we pulse pick the 160-MHz pulse trains down to 1 Hz using Mach-Zehnder modulators (MZMs) driven with FPGA-generated gating pulses. These gated, 700-fs-long (FWHM) optical pulses have the same stability as the underlying optical comb, despite nanosecond timing jitter on the gating pulses. Since direct photodetection would result in picosecond timing uncertainty, the PPS relative timing is measured optically. As shown in Fig. 2(d), we use an optical in-phase (I) and quadrature (Q) demodulator to extract the IQ signals from the interference of two PPSs [27]. The quadrature sum of the IQ can then be used to detect the temporal overlap of the PPS pulse envelopes while suppressing any impact of the optical carrier on this measurement. The quadrature signal is maximized for simultaneous arrival of the PPS optical pulses. Temporal overlap at the IQ demodulator is established with FPGA gate delays and a variable delay stage, thereby establishing a common reference plane for both PPS generators.

For sensitivity to timing shifts, we purposefully offset the PPS arrival times by 250 fs so that the measured IQ heterodyne amplitude depends linearly on the relative pulse arrival time (with a slope of ~2 ps/V) over a 325-fs range. Unfortunately, the IQ demodulator is imperfect and introduces biases associated with the relative optical phase of the two signals. We eliminate this systematic by gating a burst of 32 pulses every second, which samples all possible phase differences given by the 5-MHz carrier phase offset on the 160-MHz pulse trains. Averaging over this full 2π relative optical phase removes any biases and enables a measurement precision of 500 as. While this burst is a more complicated waveform, it is still an unambiguous timing signal. Since the comb timing noise is correlated on timescales below 1 μs [16], averaging over the burst will still yield the true pulse-to-pulse timing jitter.

Figure 2(c) shows the relative time offset in the PPS signals. The peak-to-peak wander is 265 fs with less than 1-fs wander over an hour. It appears that humidity is the main driver of the timing drifts for longer times. Laboratory humidity data correlate strongly with both PPS and optical pulse-train measurements (see Fig. 3). The dependence of timing on humidity is estimated at 13 fs per %RH for the PPS measurement and 1.5 fs per %RH for the optical pulse-train measurement. It is suspected that humidity sensitivity of out-of-loop fiber paths and other optical components are responsible for the much larger drift in the PPS signal. Other potential sources of drift such as comb power or laboratory temperature were monitored but were too small to contribute significantly.

C. 10-MHz frequency comparison

In addition to a PPS, most clocks also output a 10-MHz reference. Here, we show that straightforward rf electronics can convert the pulse train of an optically referenced comb into a highly stable 10-MHz signal. As shown in Fig. 1(a), our 10-MHz signal is generated via division of the directly photodetected, 1-mW, 160-MHz optical pulse train. We use a highly linear, 6-GHz photodiode to detect the pulse train, which is then amplified using a low-flicker-floor, 500-MHz amplifier. The pulse train is then divided with a 1/16 low-noise digital divider to generate the 10-MHz signal.

Figure 4 displays the frequency instability of the comb-generated 10-MHz signal alongside the instability of a commercial H maser. The frequency instability is quantified using the modified Allan deviation (MDEV). The 10-MHz rf generation supports a fractional frequency instability of 1.3×10^{-14} at 1 s, averaging down to 2×10^{-19}, with the instability limited largely by the noise floor of the commercial phase noise test set used for this measurement. Using a different commercial phase noise test set capable of only short-term measurements, fractional frequency instabilities could reach the $\sim 5 \times 10^{-15}$ level at 1 s (still limited by the test-set noise floor). Improved instability would be achieved by optically generating and detecting much higher microwave frequencies, but at the cost of added complexity [28]. Despite its limitations, our simple approach generates a 10-MHz signal with a relative instability exceeding that of a hydrogen maser.

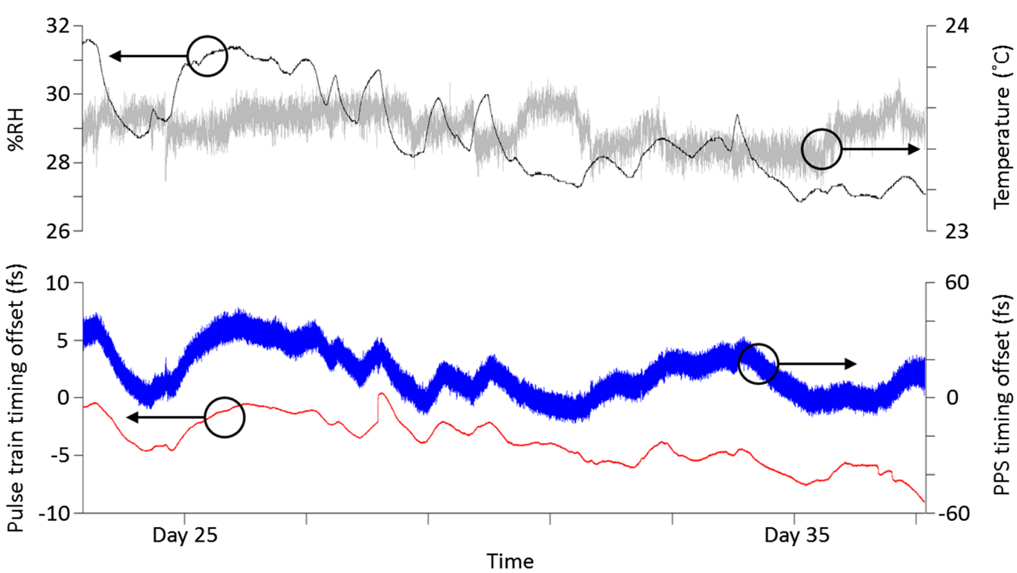

FIG. 3. Top panel: Relative humidity (%RH) (black) and temperature (gray) data for the last two weeks of timing comparison experiment during which humidity data were available. Temperature data have been smoothed with a 10-min window. Bottom panel: Pulse-train timing (red) and PPS timing (blue). The strong correlation between humidity and timing offsets is clearly evident.

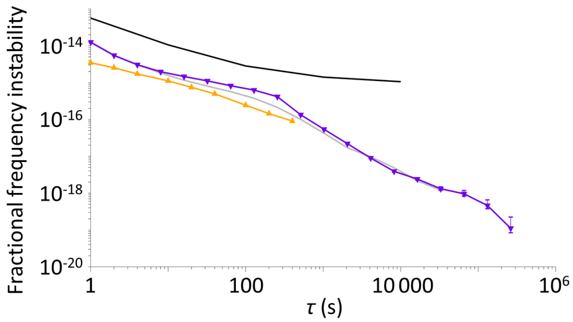

FIG. 4. Fractional frequency instability (MDEV) for our 10-MHz rf generator as measured with a test set capable of long-term operation (purple down-pointing triangle) and as measured with a low-noise test set [orange up-pointing triangle; scaled from Allan deviation (ADEV) values reported by test set]. Noise floor of the long-term test set is plotted in gray. Also shown are the MDEV values for a state-of-the-art, commercial hydrogen maser (black). A factor of $\sqrt{2}$ has been removed from the comb-generated instability data assuming an equal contribution from each clockwork.

III. DISCUSSION

In this work, we utilize a common optical oscillator in the form of a laboratory-based cavity-stabilized laser, but a future compact optical timescale would replace this oscillator with a full optical atomic clock and a robust, stabilized laser [6,7,29,30]. In Fig. 5, we compare the residual time deviations (TDEVs) for the optical time outputs of the clockwork to the absolute TDEVs for the current best optical clocks. The projected TDEVs for the optical clocks are generated by scaling reported Allan deviations, assuming white FM noise is the dominant noise source and equal contribution from both clocks [31]. These assumptions lead to an overall scaling of $\tau/\sqrt{12}$ (where τ is the averaging time) between reported clock Allan deviations and projected clock TDEVs. As expected, the relative timing of the optical pulse trains is well below the absolute TDEV of the clocks for all τ. The PPS time signals reach the optical clock level at around 60 s and hover close to or beneath the clocks for longer times. The lowest recorded TDEV for the PPS is 240 as at $\tau = 1000$ s and the lowest TDEV for the full optical pulse train is 1.5 as at $\tau = 0.5$ s.

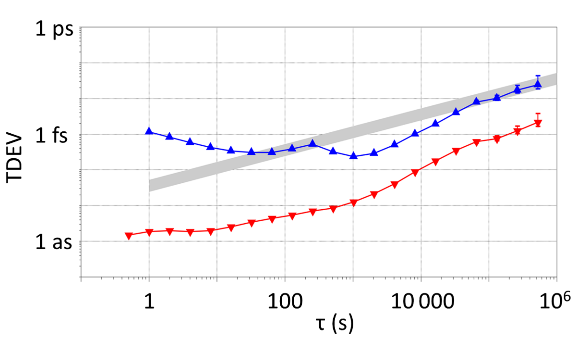

FIG. 5. Time deviation (TDEV) of the optical pulse-train timing comparison (red down-pointing triangle) and the 1 PPS timing comparison (blue up-pointing triangle) over 37 days. The gray region represents the best possible TDEV supported by current optical clocks [32,33]. Values have been divided by $\sqrt{2}$ assuming equal contribution from each comb.

While the optical PPS generation mechanism described in this paper is sufficiently stable to support current optical clocks at longer times, there are many improvements that could be made to the current system. At short times, the PPS is limited by the ~1 fs timing jitter on the combs. To improve performance at times under 100 s, one could further suppress the timing jitter of the combs with tighter locking [22,23] or with the use of an alternate waveform, such as a pulse per millisecond, which would average over more noise realizations and improve system performance at 1 s by a factor of ~30 while maintaining a very manageable ambiguity. A system with both PPS and pulse per millisecond could be easily implemented using the FPGA and MZM gate hardware. Removing out-of-loop fiber and/or actively stabilizing fiber paths would improve instability for time periods longer than 100 s. At times exceeding one month, it is likely that further engineering of the clockwork system is required for reliable operation. In addition, the use of redundant combs could relax this requirement by allowing one to intercompare and identify timing errors.

IV. CONCLUSION

Converting optical frequency references to time outputs is essential for future optical timescales. Up to now, phase coherence between the optical reference and the time output could only be maintained for hours or a few days. A reliable optical timescale, however, requires robust frequency combs capable of maintaining femtosecond-level timing over months or even years. The system described here ran slip free for over a month, with an underlying timing stability of the combs that was ~10× quieter than state-of-the-art optical clocks. Thus, our comb-based clockwork should be able to support optical clocks with no degradation of the timing signals.

ACKNOWLEDGMENTS

This material is based upon work supported by the Air Force Research Laboratory and the Defense Advanced Research Projects Agency under Contract No. F A8650-1 5-C-7 53 l. Any opinions, findings and conclusions or recommendations expressed in this material are those of the authors and do not necessarily reflect the views of the Air Force Research Laboratory or the Defense Advanced Research Projects Agency. We thank Stefania Romisch and Jeff Sherman for helpful comments.

[1] F. Riehle, Towards a redefinition of the second based on optical atomic clocks, C.R. Phys. **16**, 506 (2015).
[2] A. D. Ludlow, M. M. Boyd, J. Ye, E. Peik, and P. O. Schmidt, Optical atomic clocks, Rev. Mod. Phys. **87**, 637 (2015).

[3] H. Katori, Optical lattice clocks and quantum metrology, Nat. Photonics **5**, 203 (2011).
[4] N. R. Newbury, Searching for applications with a fine-tooth comb, Nat. Photonics **5**, 186 (2011).
[5] S. A. Diddams, The evolving optical frequency comb [Invited], J. Opt. Soc. Am. B **27**, B51 (2010).
[6] K. W. Martin, G. Phelps, N. D. Lemke, M. S. Bigelow, B. Stuhl, M. Wojcik, M. Holt, I. Coddington, M. W. Bishop, and J. H. Burke, Compact Optical Atomic Clock Based on a Two-Photon Transition, Phys. Rev. Applied **9**, 014019 (2018).
[7] T. Schuldt, K. Döringshoff, E. V. Kovalchuk, A. Keetman, J. Pahl, A. Peters, and C. Braxmaier, Development of a compact optical absolute frequency reference for space with 10^{-15} instability, Appl. Opt. **56**, 1101 (2017).
[8] N. D. Lemke, G. Phelps, J. H. Burke, K. Martin, and M. S. Bigelow, in *Proceedings of the 2017 Joint Conference of the European Frequency and Time Forum and IEEE International Frequency Control Symposium (EFTF/IFC)* (IEEE, New York, 2017), pp. 466–467.
[9] F. Riehle, Optical clock networks, Nat. Photonics **11**, 25 (2017).
[10] C. Lisdat, G. Grosche, N. Quintin, C. Shi, S. M. F. Raupach, C. Grebing, D. Nicolodi, F. Stefani, A. Al-Masoudi, S. Dörscher, S. Häfner, J.-L. Robyr, N. Chiodo, S. Bilicki, E. Bookjans, A. Koczwara, S. Koke, A. Kuhl, F. Wiotte, F. Meynadier *et al.*, A clock network for geodesy and fundamental science, Nat. Commun. **7**, 12443 (2016).
[11] J.-D. Deschênes, L. C. Sinclair, F. R. Giorgetta, W. C. Swann, E. Baumann, H. Bergeron, M. Cermak, I. Coddington, and N. R. Newbury, Synchronization of Distant Optical Clocks at the Femtosecond Level, Phys. Rev. X **6**, 021016 (2016).
[12] T. Takano, M. Takamoto, I. Ushijima, N. Ohmae, T. Akatsuka, A. Yamaguchi, Y. Kuroishi, H. Munekane, B. Miyahara, and H. Katori, Real-time geopotentiometry with synchronously linked optical lattice clocks, Nat. Photonics **10**, 662 (2016).
[13] S. A. Diddams, T. Udem, J. C. Bergquist, E. A. Curtis, R. E. Drullinger, L. Hollberg, W. M. Itano, W. D. Lee, C. W. Oates, K. R. Vogel, and D. J. Wineland, An optical clock based on a single trapped $^{199}Hg^{+}$ ion, Science **293**, 825 (2001).
[14] T. Udem, J. Reichert, R. Holzwarth, and T. W. Hänsch, Accurate measurement of large optical frequency differences with a mode-locked laser, Opt. Lett. **24**, 881 (1999).
[15] H. Inaba, Y. Daimon, F.-L. Hong, A. Onae, K. Minoshima, T. R. Schibli, H. Matsumoto, M. Hirano, T. Okuno, M. Onishi, and M. Nakazawa, Long-term measurement of optical frequencies using a simple, robust and low-noise fiber based frequency comb, Opt. Express **14**, 5223 (2006).
[16] L. C. Sinclair, J.-D. Deschênes, L. Sonderhouse, W. C. Swann, I. H. Khader, E. Baumann, N. R. Newbury, and I. Coddington, Invited article: A compact optically coherent fiber frequency comb, Rev. Sci. Instrum. **86**, 081301 (2015).
[17] H. R. Telle, B. Lipphardt, and J. Stenger, Kerr-lens, mode-locked lasers as transfer oscillators for optical frequency measurements, Appl. Phys. B **74**, 1 (2002).
[18] C. Grebing, A. Al-Masoudi, S. Dörscher, S. Häfner, V. Gerginov, S. Weyers, B. Lipphardt, F. Riehle, U. Sterr, and C. Lisdat, Realization of a timescale with an accurate optical lattice clock, Optica **3**, 563 (2016).
[19] T. Ido, H. Hachisu, F. Nakagawa, and Y. Hanado, Rapid evaluation of time scale using an optical clock, J. Phys. Conf. Ser. **723**, 012041 (2016).
[20] L. C. Sinclair, I. Coddington, W. C. Swann, G. B. Rieker, A. Hati, K. Iwakuni, and N. R. Newbury, Operation of an optically coherent frequency comb outside the metrology lab, Opt. Express **22**, 6996 (2014).
[21] J. Lee, K. Lee, Y.-S. Jang, H. Jang, S. Han, S.-H. Lee, K.-I. Kang, C.-W. Lim, Y.-J. Kim, and S.-W. Kim, Testing of a femtosecond pulse laser in outer space, Sci. Rep. **4**, 5134 (2014).
[22] N. Kuse, C.-C. Lee, J. Jiang, C. Mohr, T. R. Schibli, and M. E. Fermann, Ultra-low noise all polarization-maintaining Er fiber-based optical frequency combs facilitated with a graphene modulator, Opt. Express **23**, 24342 (2015).
[23] M. Lezius, T. Wilken, C. Deutsch, M. Giunta, O. Mandel, A. Thaller, V. Schkolnik, M. Schiemangk, A. Dinkelaker, A. Kohfeldt, A. Wicht, M. Krutzik, A. Peters, O. Hellmig, H. Duncker, K. Sengstock, P. Windpassinger, K. Lampmann, T. Hülsing, T. W. Hänsch, and R. Holzwarth, Space-borne frequency comb metrology, Optica **3**, 1381 (2016).
[24] E. Baumann, F. R. Giorgetta, J. W. Nicholson, W. C. Swann, I. Coddington, and N. R. Newbury, High-performance, vibration-immune fiber-laser frequency comb, Opt. Lett. **34**, 638 (2009).
[25] D. R. Leibrandt and J. Heidecker, An open source digital servo for atomic, molecular, and optical physics experiments, Rev. Sci. Instrum. **86**, 123115 (2015).
[26] D. Hou, C.-C. Lee, Z. Yang, and T. R. Schibli, Timing jitter characterization of mode-locked lasers with $<1\ \mathrm{zs}/\sqrt{\mathrm{Hz}}$ resolution using a simple optical heterodyne technique, Opt. Lett. **40**, 2985 (2015).
[27] L. G. Kazovsky, L. Curtis, W. C. Young, and N. K. Cheung, All-fiber 90° optical hybrid for coherent communications, Appl. Opt. **26**, 437 (1987).
[28] F. N. Baynes, F. Quinlan, T. M. Fortier, Q. Zhou, A. Beling, J. C. Campbell, and S. A. Diddams, Attosecond timing in optical-to-electrical conversion, Optica **2**, 141 (2015).
[29] D. R. Leibrandt, M. J. Thorpe, J. C. Bergquist, and T. Rosenband, Field-test of a robust, portable, frequency-stable laser, Opt. Express **19**, 10278 (2011).
[30] S. Vogt, C. Lisdat, T. Legero, U. Sterr, I. Ernsting, A. Nevsky, and S. Schiller, Demonstration of a transportable 1 Hz-linewidth laser, Appl. Phys. B **104**, 741 (2011).
[31] S. T. Dawkins, J. J. McFerran, and A. N. Luiten, Considerations on the measurement of the stability of oscillators with frequency counters, IEEE Trans. Ultrason. Ferroelectr. Freq. Control **54**, 918 (2007).
[32] I. Ushijima, M. Takamoto, M. Das, T. Ohkubo, and H. Katori, Cryogenic optical lattice clocks, Nat. Photonics **9**, 185 (2015).
[33] M. Schioppo, R. C. Brown, W. F. McGrew, N. Hinkley, R. J. Fasano, K. Beloy, T. H. Yoon, G. Milani, D. Nicolodi, J. A. Sherman, N. B. Phillips, C. W. Oates, and A. D. Ludlow, Ultrastable optical clock with two cold-atom ensembles, Nat. Photonics **11**, 48 (2017).